Optical Properties of *N*-Succinimidyl Bithiophene and the Effects of the Binding to Biomolecules: Comparison between Coupled-Cluster and Time-Dependent Density Functional Theory Calculations and Experiments

E. Fabiano,[†] F. Della Sala,*[,†] G. Barbarella,[‡] S. Lattante,[†,§] M. Anni,[†,||] G. Sotgiu,[‡] C. Hättig,[⊥] R. Cingolani,[†] and G. Gigli[†,||]

National Nanotechnology Laboratory of INFM-CNR, Distretto Tecnologico, Università degli Studi di Lecce, Via per Arnesano, I-73100 Lecce, Italy, ISOF, Area della Ricerca CNR, Via Gobetti 101, I-40129 Bologna, Italy, Dipartimento di Fisica, Università degli Studi di Lecce, Via per Arnesano, I-73100 Lecce, Italy, Dipartimento di Ingegneria dell'Innovazione, Università degli Studi di Lecce, Via per Arnesano, I-73100 Lecce, Italy, and Lehrstuhl für Theoretische Chemie, Ruhr-Universität Bochum, Universitätsstrasse 10, D-44780 Bochum, Germany

Received: May 11, 2006; In Final Form: July 20, 2006

We report a joint theoretical−experimental study on the optical properties of 5-*N*-succinimidyl-2,2′-bithiophene (NS-2T), a prototype system for a new class of biomarkers. Time-dependent density functional theory (TD-DFT) and approximate coupled-cluster single and doubles (CC2) calculations are performed in the ground and excited states. Theoretical results are compared with absorption, photoluminescence (PL), time-resolved PL, and PL quantum efficiency measurements. The excited state of NS-2T has a larger dipole moment as compared to that of the ground state, explaining the experimental shift of the PL peak in solvents of different polarity, and a smaller intersystem crossing (ISC) rate as compared to that of isolated bithiophene (2T), explaining the increased PL quantum efficiency. We also studied two model systems to describe the effects of the covalent binding of NS-2T to biomolecules and proteins with the ϵ-NH_2 lysine groups. These model systems show optical properties closer to 2T, as the PL quantum efficiency is reduced due to the increased ISC rate. Theoretical calculations and experimental results show that covalent binding of NS-2T to a biomolecule will blue-shift the absorption but not the photoluminescence. CC2 and TD-DFT can very well describe the absorption and photoluminescence energies of all three systems, but the presence of several charge-transfer transitions in the TD-DFT spectrum of NS-2T required the use of a correlated method to validate the TD-DFT results.

I. Introduction

Fluorescence labeling is a widely used tool in biology and medical diagnosis, and it will probably replace conventional techniques based on radioisotopes soon. Fluorescence techniques have opened new possibilities for molecular and cellular imaging and for the monitoring of biological processes. The development of new and more efficient fluorescent probes is actually an issue of great interest in many areas of research.[1−11]

Recently great attention has been paid to the use of organic compounds as fluorescent probes.[3−6,9] Many organic compounds can be identified that have suitable optical properties and that can be easily functionalized to allow binding to biomolecules. Unfortunately the functionalization and the binding to biomolecules might change the optical and photophysical behavior of the probes and make them unsuited for use as fluorescent labels. Therefore a careful investigation is required to study the effect of functionalization, first, and of binding on the photophysical and optical properties of the molecule, before it can be used as a probe in fluorescent experiments.

In a recent work[12] the oligothiophene *N*-succinimidyl esters (TSEs) have been introduced. These molecules are derived from oligothiophenes,[13] which have been already successfully used in many electronic and optoelectronic applications, such as organic light-emitting diodes,[14,15,16,17] lasers,[18] and field-effect transistors.[19−21] TSEs have shown, after the binding with proteins or oligonucleotides, high fluorescence efficiency, good optical stability, large Stokes shifts, and good color tunability and have been successfully employed to obtain fluorescence microscopy images and in fluorescence resonance energy transfer experiments. These features, along with the easy synthesis and the easy modalities of binding to oligonucleotides and proteins, make the TSEs one of the best classes of organic fluorescent markers.

In this work we study in detail the photophysical and optical properties of the TSEs, both theoretically and experimentally, and consider the modifications in the electronic structure of the molecule when it is bound to a biomolecule. As a prototype of the complete TSE class, we have investigated the 5-*N*-succinimidyl-2,2′-bitiophene (NS-2T, see the top of Figure 1), which is the smallest member of the family.

Concerning the bioconjugation, it is known that the *N*-succinimidyl ester reacts with the ϵ-NH_2 lysine groups of

* Author to whom correspondence should be addressed. E-mail: fabio.dellasala@unile.it.
† National Nanotechnology Laboratory of INFM-CNR, Università degli Studi di Lecce.
‡ ISOF, Area della Ricerca CNR.
§ Dipartimento di Fisica, Università degli Studi di Lecce.
|| Dipartimento di Ingegneria dell'Innovazione, Università degli Studi di Lecce.
⊥ Lehrstuhl für Theoretische Chemie, Ruhr-Universität Bochum.

10.1021/jp062890w CCC: $33.50
Published on Web 08/30/2006

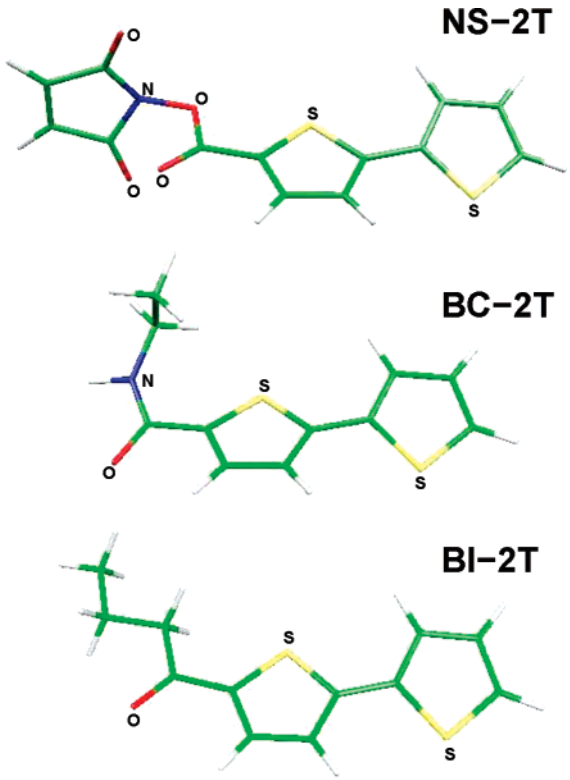

Figure 1. The 5-*N*-succinimidyl-2,2′-bitiophene (NS-2T) molecule and the bioconjugate BC-2T and BI-2T models.

proteins, forming a stable amine bond.[22,23] Thus, we can consider for the NS-2T (here explicitly denoted as 2T−C(O)−O−NS) the following binding reaction

$$2T-C(O)-O-NS + NH_2-\text{protein} \rightarrow 2T-C(O)-NH-\text{protein}$$

Therefore, taking a CH_2CH_3 group as representative of the terminal part of a protein, we can model the covalent binding to a biomolecule. To study such covalent binding we synthesized, measured, and computed a bithiophene bearing a C(O)−NH−CH_2−CH_3 group at one terminal position, hereafter called BC-2T. In addition, to clarify the role played by the NH and C−O groups in the linker, we considered a bithiophene bearing a C(O)−CH_2−CH_2−CH_3 group at one end, named BI-2T.

Preliminary calculations of the optical properties of *N*-succinimidyl bitiophene[12] showed the importance of charge-transfer (CT) contributions. To describe the charge-transfer character of excited states an accurate correlated method is required, such as the coupled-cluster method.[24] The coupled-cluster method is a post-Hartree−Fock (HF) size-consistent method that provides an accurate description of excited states and can also be used for high-level optimization of ground-state and excited-state geometries. In particular the optical properties of systems of the size of TSEs can be efficiently studied using the approximate coupled-cluster singles and doubles model (CC2)[25] together with the resolution-of-identity (RI) approximation, which has already been successfully employed for the calculation of the excitation energies of large π-conjugated molecules[26−28] and for the geometry optimization of both ground and excited states of a variety of many different systems.[29,30]

However, time-dependent density-functional theory (TD-DFT), which is the most commonly used approach to deal with the excited states of organic molecules, must be used with caution for the computation of excitations of TSEs, and the results must be accurately checked to avoid artifacts due to the well-known limitations of TD-DFT in treating charge-transfer systems.[31−38] In fact, when applied to the calculation of excitations involving charge transfer between widely separated species within a molecule, TD-DFT yields severely underestimated results for the charge-transfer excitation energies.[33] This failure is due to the local character of the approximate exchange−correlation (XC) functional, and TD-DFT cannot yield correct CT states with any local XC functional.[33] Although the use of a simple hybrid kernel such as B3LYP[39] can improve the quality of charge-transfer excitation energies in the case of short CT separation,[32,33,40] it yields an incorrect long-range behavior. Several approaches have been proposed to solve the CT problem;[31,33,36,37] however, these approaches are only approximate and still require external calculations[31,33] or parameters,[37,36] and thus these methods cannot compete with CC2 in describing CT excitation energies.

In this work, we studied the absorption spectra of the NS-2T, BC-2T, and BI-2T molecules experimentally and by CC2 and TD-DFT calculations to obtain a clear picture of singlet and triplet excitations in the three systems and to test the ability of TD-DFT to describe such excitations. We use the common B3LYP XC functional, and compare the excitation energies with those of CC2. Absorption spectra measurements are carried out in solvents of different polarities to investigate the effects of the electronic dipole moment. Then we calculated the emission spectra of the three systems and compared the results with the PL experimental values. The emission spectra were obtained by optimizing the geometry of the optically active excited state, by a recently developed TD-DFT method.[41] By calculation of the singlet and triplet spectra at the correct, i.e., excited-state minimum, geometry semiquantitative analysis of the photophysical properties of these molecules can be obtained and compared to nonradiative decay rates extracted from time-resolved PL and PL quantum efficiency (PLQE) measurements.[42]

The article is organized as follows: In section II, the computational details and the experimental setup are described. In section III, we illustrate the results of calculations and experiments. Then, in section IV, theoretical results of different methods are compared with each other and with experiments; moreover a comparison between the various systems is carried out. Finally, in section V, conclusions are drawn.

II. Method

A. Computational Details. The geometry optimization of the ground states of NS-2T, BC-2T, and BI-2T was carried out using the approximate coupled-cluster singles and doubles method (CC2)[25] with the resolution-of-identity (RI) approximation (RI-CC2[25,43]) in the TZVPP[44,45] basis set.

We also optimized the geometry of the optically active excited states of NS-T2 and BC-T2, using the computationally much less demanding TD-DFT[41] with the B3LYP[39] hybrid kernel and the triple-ζ valence basis set (TZVP).[45]

To verify the quality of the TD-DFT excited-state geometry, we computed for NS-2T the excited-state geometry using the CC2 method and the TZVPP basis set, and we analyzed the CC2 singlet and triplet spectra computed with the two geometries. Using the TD-DFT geometry, we found that the spectrum is only blue-shifted by less than 0.1 eV, meaning that the TD-DFT excited-state geometry can be used. We note that all the results reported in this work for excited-state geometries were obtained at the geometries optimized with TD-DFT.

The state selected for the excited-state geometry optimization was the optically active one, which for NS-T2 is not the lowest (section III). During the optimization, it crosses with lower states. By analyzing the oscillator strengths of the two, we could resolve the crossing and follow the optically active state in the final excited-state conformation.

From ground-state geometries, vertical singlet excitation energies were calculated, using the RI-CC2 method, to obtain information about the absorption spectrum. The Dunning triple-ζ valence basis set with augmented functions (aug-cc-pVTZ),[46] which has been shown to be large enough to obtain converged CC2 results on oligothiophenes,[28] was used. The corresponding auxiliary basis set[47] was used to exploit the RI approximation, and in all CC2 calculations the core orbitals have been kept frozen. RI-CC2 calculations were well converged and did not suffer from the possible multireference nature of the ground state of the systems investigated (D1 diagnostic[48] values in the range of 0.07−0.08) and from the neglect of triple or higher excitations (single excitation contribution always greater than 90%).

We also calculated TD-DFT vertical singlet excitations of NS-2T, BC-2T, and BI-2T in the ground-state configuration. We used the TZVP[45] basis set and B3LYP functional[39] to take advantage of the nonlocal HF exchange, especially in consideration of the charge-transfer nature of some of the single-particle transitions of the investigated systems.

For NS-2T (Figure 9), we also compare three different XC functionals using the XCU1T[51] basis set: B3LYP, Becke−Perdew,[49,50] and the LHFX approach,[54] i.e., the localized Hartree−Fock approach to obtain self-interaction-free Kohn−Sham orbitals and eigenvalues[52,53] combined with a TD-DFT calculation that employs the Becke exchange kernel.[49]

From TD-DFT excited-state geometries, we computed vertical CC2 singlet and triplet excitation energies using the aug-cc-pVTZ basis set.

All the calculations were performed with the quantum-chemistry program package TURBOMOLE V5.7.[55] In particular the modules DSCF,[56−58] RELAX,[59] ESCF,[60−64] and RI-CC2[26,29,65−67] were used. Parallel RI-CC2 calculations have been performed on a Hewlett-Packard XC6000 Itanium2 Cluster.

B. Experimental Setup. Solutions were prepared with spectroscopic grade solvents without further purification. To avoid intermolecular interactions the concentration was decreased down to about 10^{-4} M. To study the effects of the environment polarity, we used three different solvents, namely, toluene, dichloromethane, and dimethyl sulfoxide (DMSO).

Continuous wave photoluminescence (PL) measurements have been performed with a Cary Eclipse Spectrofluoremeter by exciting the solutions at 325 nm with a lamp.

The PL quantum efficiency was determined by comparing the samples integrated PL intensity with that of dithienothiophene-4,4-dioxide (efficiency 61% in tetrahydrofurane[68]) solutions with the same optical density at the excitation wavelength. The signal was corrected considering the differences of the refractive index of the employed solvents. The absorption spectra were measured with a double-beam spectrophotometer.

Time-resolved PL measurements were performed by exciting the samples with the second harmonic (390 nm) of a mode-locked Ti−sapphire (Spectra Physics Tsunami), delivering 80 fs pulses with a repetition rate of 80 MHz. The signal was dispersed in wavelength and time by a spectrometer coupled with a Hamamatsu C5680 streak camera. The overall temporal resolution was about 10 ps.

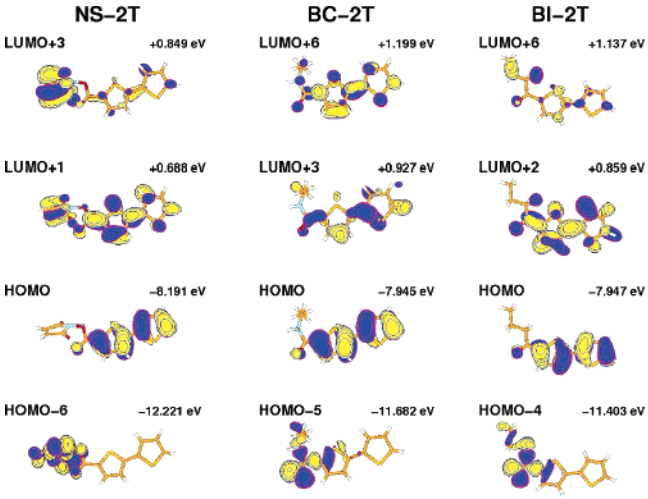

Figure 2. Most relevant HF orbitals and eigenvalues in the ground-state geometry.

TABLE 1: Lowest Three Singlet Excitation Energies (eV) with Oscillator Strengths (in Parentheses) and Main Single-Particle Transitions of NS-2T as Computed at the CC2 and TD-DFT Levels

	CC2			TD-DFT		
	energy	transition	%	energy	transition	%
S_1	3.64 (0.00)	H − 6 → L + 3	66.4	2.74 (0.01)	H → L	99.3
		H − 6 → L + 1	20.2			
S_2	3.91 (0.70)	H → L + 1	75.6	3.38 (0.00)	H − 3 → L	88.0
		H → L + 3	9.9			
S_3	4.14 (0.01)	H − 5 → L + 3	29.8	3.55 (0.63)	H → L + 1	97.5
		H − 4 → L + 3	20.8			
		H − 9 → L + 3	12.1			

III. Results

A. Theoretical Results. *1. Geometries.* In the ground state, the optimized geometry of the bithiophene segment of NS-2T is very similar to that of isolated bithiophene.[72] The inter-ring distance is 1.44, Å and the dihedral angle between the two rings is 23°. The distance between the carbon atom in the C−O group and the nearest thiophene ring is 1.45 Å. The *N*-succinimidyl group is almost perpendicular to the nearest thiophene ring.

Upon excitation in the first optically active singlet state the bithiophene segment of the molecule acquires a quinoid character and becomes planar while the *N*-succinimidyl group is left almost unchanged. This behavior is due to the localization of the transition density on the bithiophene segment of the molecule (sect. IV).

The substitution of the *N*-succinimidyl group with C(O)−CH_2−CH_2−CH_3 (BI-2T) or C(O)−NH−CH_2−CH_3 (BC-2T) does not change, in the ground state, the geometry of the bithiophene. In BC-2T only, the torsional angle is increased to 25°. The distance of the added group from the nearest thiophene ring is, in both cases, much larger than that in NS-2T with bond lengths of 1.47 and 1.48 Å for BI-2T and BC-2T, respectively.

2. Excitation Energies. Calculated singlet excitation energies of NS-2T are reported in Table 1. The HF orbitals most relevant for the analysis of excitation energies are reported in Figure 2.

The optically active state, at the CC2 level of computation, is the second singlet state, which is mainly described a transition from the highest occupied molecular orbital (HOMO) to the second lowest unoccupied molecular orbital (LUMO + 1); single-particle transition will be indicated in the following as, e.g., HOMO → LUMO + 1. The HOMO is essentially localized on the two thiophene rings and closely resembles the HOMO

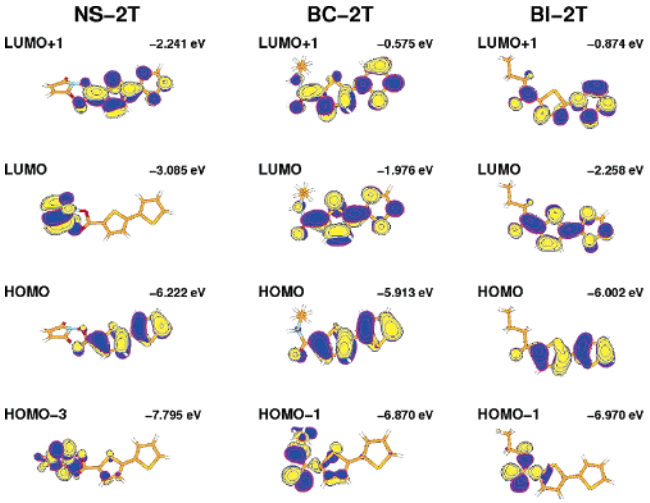

Figure 3. Most relevant DFT orbitals and eigenvalues in the ground-state geometry.

of bithiophene;[28] the LUMO + 1 is instead delocalized on the whole molecule. The excited state also has a signature from the HOMO → LUMO + 3 transition, which is an almost pure (i.e., with no overlap between involved orbitals) CT transition because the LUMO + 3 is localized on the succinimidyl group. The S_1 state is instead a dark state (i.e., with vanishing oscillator strength), and it is mainly described by a HOMO − 6 → LUMO + 3 transition; this is a transition concerning orbitals all localized on the succinimidyl group. There is again a non-negligible contribution coming from the HOMO − 6 → LUMO + 1 (20.2%) transition. The third singlet state is a dark state characterized by an admixture of many single-particle transitions.

The TD-DFT results in Table 1 are, at a first sight, quite different from the CC2 ones. Nevertheless, a closer inspection reveals many similarities. If we exclude, as it will be explained in section IV, the excitations characterized by the HOMO → LUMO transition, which have no analogous excitations in the CC2 spectrum, then we find that the optically active state (S_3) is now the *second* singlet state, as in the CC2 results. It is characterized by a HOMO → LUMO + 1 transition, which is localized mainly on the bithiophene (Figure 3). The TD-DFT S_2 state is characterized by a HOMO − 3 → LUMO transition, which is mainly localized on the succinimidyl group. These transitions are closely related, in terms of orbital densities, to the HOMO → LUMO + 1 (plus HOMO → LUMO + 3) and HOMO − 6 → LUMO + 3 (plus HOMO − 6 → LUMO + 1) transitions with HF orbitals, respectively. Thus, we can recognize a one-to-one correspondence between the TD-DFT and CC2 results for the lowest singlet states; also the CC2 values for the vertical excitation energies are about 0.3 eV higher.

In Table 2 we report the calculated absorption energies for BC-2T.

The CC2 calculations predict the first singlet state to be the active state. This is described by an admixture of several transitions, the principal ones being HOMO → LUMO + 6 and HOMO → LUMO + 3. These are transitions among orbitals localized on the bithiophene rings. The HOMO is almost identical to the HOMO of NS-2T. The LUMO + 6 and LUMO + 3 are mainly localized on single bonds and on sulfur atoms, in close analogy to the LUMO of isolated bithiophene.[28] The higher singlets are all optically forbidden and described by an admixture of many single-particle transitions.

The B3LYP results essentially reproduce CC2 calculations. The lowest singlet state is the active state. It is described by a

TABLE 2: Lowest Three Singlet Excitation Energies (eV) with Oscillator Strengths (in Parentheses) and Main Single-Particle Transitions for BC-2T as Computed at the CC2 and TD-DFT Levels

	CC2			TD-DFT		
	energy	transition	%	energy	transition	%
S_1	4.05 (0.56)	H → L + 6	32.0	3.68 (0.54)	H → L	97.2
		H → L + 3	16.2			
		H → L + 4	13.9			
S_2	4.37 (0.03)	H − 5 → L + 6	17.8	4.07 (0.01)	H − 1 → L	72.6
		H − 5 → L + 3	9.6		H − 2 → L	15.8
S_3	4.82 (0.00)	H − 1 → L + 6	13.3	4.53 (0.01)	H − 2 → L	61.9
					H − 1 → L	19.1
					H → L + 1	10.0

TABLE 3: Lowest Three Singlet Excitation Energies (eV) with Oscillator Strengths (in Parentheses) and Main Single-Particle Transitions for BI-2T as Computed at the CC2 and TD-DFT Levels

	CC2			TD-DFT		
	energy	transition	%	energy	transition	%
S_1	3.72 (0.01)	H − 4 → L + 2	49.5	3.51 (0.24)	H − 1 → L	50.0
					H → L	44.1
S_2	3.92 (0.64)	H → L + 2	72.8	3.55 (0.33)	H → L	53.7
					H − 1 → L	41.2
S_3	4.69 (0.01)	H − 2 → L + 2	23.7	4.44 (0.01)	H − 2 → L	51.9
		H − 1 → L + 2	21.7		H → L + 1	34.9
		H → L + 16	16.1			

HOMO → LUMO transition, whose change in electronic density is quite similar to the admixture HOMO → LUMO + 6 and HOMO → LUMO + 3 found in CC2 calculations. The higher singlets are dark states described by many single-particle transitions.

We note that in both CC2 and in TD-DFT calculations only singlet excitations dominated by a bithiophene → bithiophene transition are optically coupled to the ground state, while excitations dominated by a succinimidyl → succinimidyl transition are optically forbidden. This is true, in general, also for BC-2T. Thus, the optically active state of NS-2T is the second singlet state, and the first singlet state has a very low oscillator strength, while in BC-2T the optically active state is the first singlet and the second singlet state is a dark state.

Finally, the calculations on BI-2T in the ground-state geometry are reported in Table 3.

The CC2 calculations give the second singlet state as the optically active state. This is well described by a HOMO → LUMO + 2 transition, the HOMO being very similar to the bithiophene HOMO and the LUMO + 2 being mainly localized on the bithiophene segment. The first singlet state is a dark state characterized by a HOMO − 4 → LUMO + 2 transition. The HOMO − 4 is mainly localized on the $C(O)-CH_2-CH_2-CH_3$ group.

The TD-DFT results mainly confirm the CC2 findings with the notable exception that the first and the second singlet states (composed of HOMO → LUMO and HOMO − 1 → LUMO with similar weight) are almost degenerate. The oscillator strengths are then redistributed between these two states.

3. Emission Energies. CC2 singlet excitation energies of NS-2T at the TD-DFT excited-state geometry are reported in Table 4. We also report the TD-DFT emission energy, which is about 0.3 eV lower than the CC2 value. The S_1 state is almost a pure HOMO → LUMO transition, localized on bithiophene (see the orbitals in Figure 4). This is the only optically active state, while the higher singlets have negligible oscillator strengths. In the ground-state conformation, the optically active state showed also a non-negligible contribution from the HOMO → LUMO + 3

TABLE 4: Singlet and Triplet Excitation Energies (eV), Oscillator Strengths (OS), and Main Single-Particle Transitions for NS-2T as Computed at the CC2 Level in the Excited-State Geometry

state	energy	OS	transitions	%
S_1	3.41(3.13[a])	0.72	H → L	92.4
S_2	3.73	0.00	H − 6 → L + 5	87.9
S_3	4.41	0.00	H → L + 5	43.5
			H − 2 → L	17.0
			H → L + 15	10.0
T_1	2.18		H → L	91.5
T_2	3.69		H − 3 → L	24.8
			H → L + 15	19.9
			H → L + 13	16.3
T_3	3.70		H − 4 → L + 5	88.8
T_4	4.00		H − 1 → L	62.1
			H − 2 → L	16.9

[a] TD-DFT result.

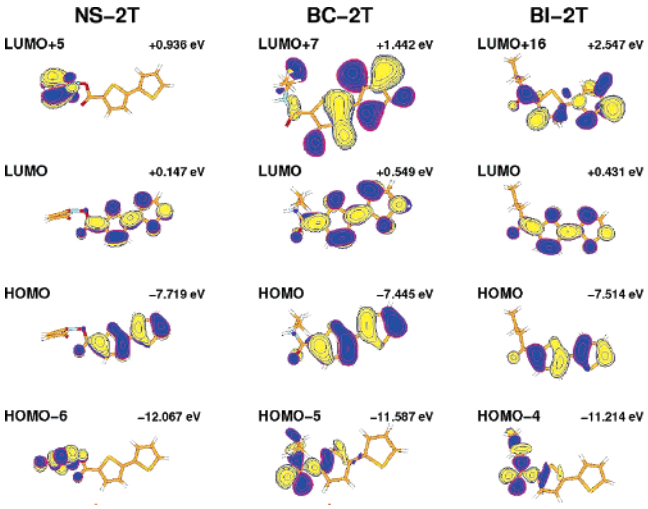

Figure 4. Most relevant HF orbitals and eigenvalues in the excited-state geometry.

transition, but this transition (which is equivalent to HOMO → LUMO + 5 in the excited state) does not give a relevant contribution here because its single-particle energy is now much larger than that of the HOMO → LUMO transition and this prevents the two transitions from mixing. Indeed the HOMO → LUMO + 5 transition is completely decoupled from the HOMO → LUMO transition, and it gives rise to the third singlet state, lying in fact about 1 eV above the first singlet state.

The S_2 state is characterized by the HOMO − 6 → LUMO + 5 transition localized on the succinimidyl group (see the orbitals in Figure 4). This excited state is thus completely equivalent to the first singlet state in the ground-state geometry as also suggested by the fact that the two excited states have very close energies. Thus, we note that the S_1 and S_2 states are interchanged with respect to the results in the ground state in Table 1. This is due to the geometry changes in the excited state, which are localized on the bithiophene and thus decrease the energy of the optically active state while excitation energies on the succinimidyl group are left almost unchanged. In the excited-state geometry, there is a strong reduction of the HOMO−LUMO gap that also brings about a reorganization of the orbitals. The shape of the HOMO is almost unchanged while its energy increases 0.47 eV. The energy of the first non-Rydberg virtual orbital (LUMO + 1 in the ground-state geometry) is reduced by 0.54 eV in the excited-state geometry, so that it becomes the LUMO, and the orbital density is more localized on the bithiophene. However, orbitals localized on the succinimidyl group are almost unchanged in shape and eigenvalues.

TABLE 5: Singlet and Triplet Excitation Energies (eV), Oscillator Strengths (OS), and Main Single-Particle Transitions for BC-2T as Computed at the CC2 Level in the Excited-State Geometry

state	energy	OS	transition	%
S_1	3.41(3.11[a])	0.56	H → L	84.6
S_2	4.04	0.04	H − 5 → L	50.9
S_3	4.44	0.00	H − 1 → L	41.9
			H → L + 7	15.8
T_1	2.15		H → L	85.6
T_2	3.61		H − 3 → L + 1	20.9
			H → L + 7	17.1
T_3	3.96		H − 5 → L	31.9
			H − 4 → L	12.7
T_4	4.10		H − 1 → L	59.7
			H − 3 → L	14.7

[a] TD-DFT result.

TABLE 6: Singlet and Triplet Excitation Energies (eV), Oscillator Strengths (OS), and Main Single-Particle Transitions for BI-2T as Computed at CC2 Level in the Excited-State Geometry

state	energy	OS	transition	%
S_1	3.40(3.09[a])	0.66	H → L	90.1
S_2	3.44	0.01	H − 4 → L	66.4
S_3	4.35	0.00	H − 1 → L	32.8
			H → L + 16	27.0
			H − 2 → L	11.4
T_1	2.13		H → L	89.1
T_2	3.22		H − 4 → L + 1	62.6
			H − 4 → L + 16	11.1
T_3	3.60		H → L + 16	34.4
			H − 3 → L	21.5
T_4	4.06		H − 1 → L	62.0
			H − 3 → L	20.2

[a] TD-DFT result.

Table 4 also includes triplet excitation energies, which will be used in section IV.C for a qualitative description of photophysical properties. The first triplet state is almost a pure HOMO → LUMO transition, while the second triplet state lies at energies higher than the active singlet state.

In Table 5 we report the singlet and triplet emission energies of BC-2T.

CC2 and TD-DFT emission energies are almost identical to the NS-2T ones. The S_1 state is the optically active state as it was in the ground state. However in the ground state (Table 2) the S_1 state single-particle transitions were spread over many unoccupied orbitals, while in the excited state it is an almost pure HOMO → LUMO transition. We note that in the excited-state geometry the electronic structure of BC-2T is only slightly modified with respect to the ground-state configuration. The main consequence is that because of the greater localization of virtual orbitals on the bithiophene, in contrast with NS-2T TD-DFT calculations, there are no artifacts in the BC-2T TD-DFT spectrum and the optically active state is the first singlet state.

Concerning the triplet spectrum, it is similar to that of NS-2T, but the T_2 excitation energy is about 0.1 eV lower than that in NS-2T.

Table 6 reports singlet and triplet emission energies of BI-2T.

Again no differences in emission energies are found as compared to NS-2T and BC-2T. However in this system the S_1 and S_2 states are almost degenerate. We also note that in the

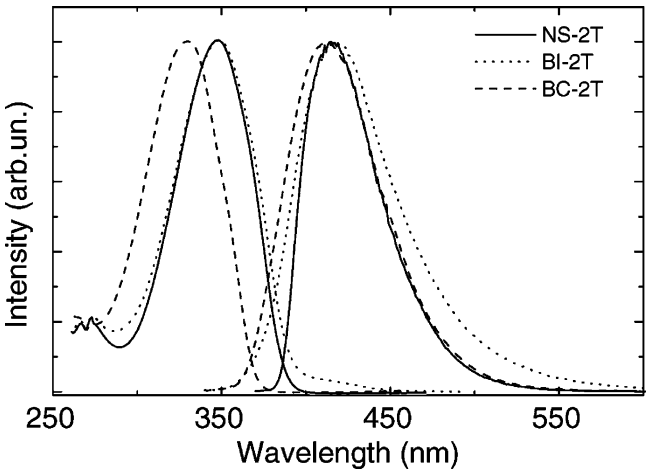

Figure 5. Absorption and PL spectra of the three molecules in dichloromethane solutions.

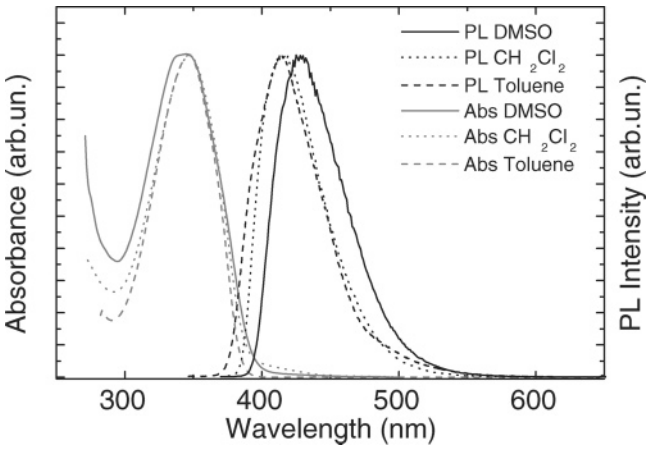

Figure 6. Absorption and PL spectra for NS-T2 in DMSO, dichloromethane, and toluene solutions.

TABLE 7: Absorption and PL Energies of the Main Peak for the Three Systems in Dichloromethane Solution

system	absorption	PL
NS-2T	348 nm (3.56 eV)	416 nm (2.97 eV)
BC-2T	330 nm (3.75 eV)	412 nm (3.01 eV)
BI-2T	348 nm (3.56 eV)	419 nm (2.95 eV)

ground state S_1 and S_2 were very close, also at the TD-DFT level. Here the S_1 state is an almost pure HOMO → LUMO transition while the S_2 state is dominated by a HOMO − 4 → LUMO one. The reason is the absence of the oxygen atom in the substituent, which increases the energy of the HOMO − 4 by 0.37 eV with respect to the corresponding orbital (HOMO − 5) in BC-2T. As a consequence the energy of the HOMO − 4 → LUMO transition and thus of the S_2 state is reduced.

The triplet spectrum is also quite different from those of the other systems. The T_2 state, which is dominated by transition out of the HOMO − 4, has much lower energy, and it is below the first singlet state.

B. Experimental Results. *1. Optical Properties.* In Figure 5 we report the absorption (Abs) and the PL spectra in dichloromethane for all the molecules.

All the spectra are characterized by one main broad peak and no evident vibrational replicas. The values of the main PL and Abs peaks are reported in Table 7. A significant shift in absorption is present between BC-2T and NS-2T while the latter is very similar to BI-2T. No significant differences (a few nanometers) are found in the PL among all the systems.

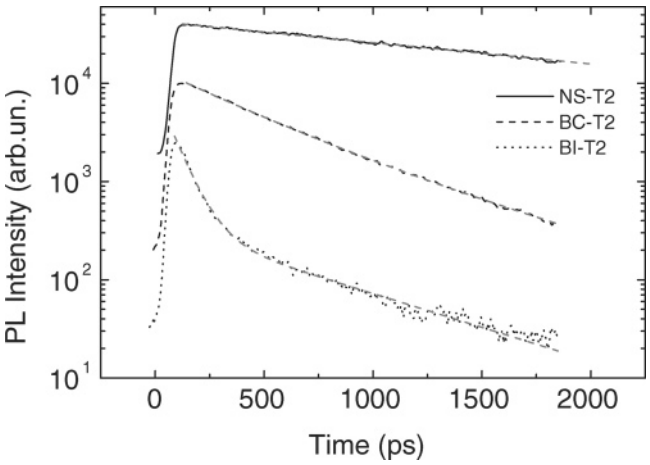

Figure 7. Photoluminescence relaxation dynamics of NS-2T, BC-2T, and BI-2T in dichloromethane solutions.

TABLE 8: Absorption and PL Energies of the Main Peak of NS-T2 in DMSO, Dichloromethane, and Toluene[a]

solvent	ϵ	dipole moment	absorption	PL
DMSO	46.7	4.1	343 nm (3.61 eV)	429 nm (2.89 eV)
CH_2Cl_2	8.9	1.1	348 nm (3.56 eV)	425 nm (2.92 eV)
toluene	2.4	0.4	347 nm (3.57 eV)	414 nm (2.99 eV)

[a] The dielectric constants (ϵ) and dipole moments (D) of the solvents are also reported.

TABLE 9: PL Quantum Efficiency (η) and Decay Times (PL, Radiative, and Nonradiative) for NS-2T, BC-2T, and BI-2T

system	η	τ_{PL}	τ_{rad}	τ_{nr}
NS-2T	28%	1.98 ns	7.2 ns	2.7 ns
BC-2T	5%	0.48 ns	8.7 ns	0.5 ns
BI-2T	1%			

TABLE 10: Dipole Moments (D) for NS-T2 in the Ground and Optically Active Excited States at the CC2 and DFT Levels

	CC2	DFT
ground state	0.508	0.703
excited state	2.420	2.913

We have also investigated the solvent dependence of the optical properties for NS-2T. The Abs and PL spectra of NS-2T in toluene, dichloromethane, and DMSO are shown in Figure 6. Some small shifts can be seen in the PL spectra. In Table 7 the dielectric constant and the dipole moment of the solvent are reported together with the wavelengths of the Abs and PL peaks.

We observe that an increase of the solvent dielectric constant from 2.4 to 46.7 leads to a red shift of the NS-2T PL peak energy by about 100 meV.

2. Photophysical Properties. In Figure 7 we report the time-resolved PL signal for NS-2T, BC-2T, and BI-2T in dichloromethane solutions. The decays are monoexponential, so that PL decay times (τ_{PL}) of NS-2T and BC-2T can be extracted, while non-monoexponential relaxation is observed for BI-T2 solutions.

In Table 9 we report the measured PLQE (η) and the corresponding radiative (τ_{rad}) and nonradiative decay times (τ_{nr}).

These decays times can be extracted from the relations

$$1/\tau_{PL} = 1/\tau_{rad} + 1/\tau_{nr} \quad \eta = \tau_{PL}/\tau_{rad}$$

The PLQE and τ_{PL} of BC-T2 are significantly smaller than those

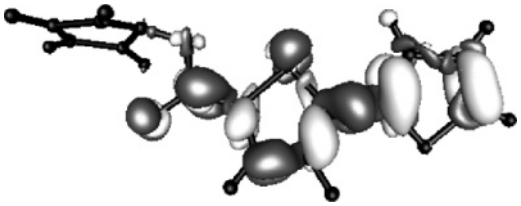

Figure 8. CC2 differential density for the optically active excited state in the ground-state geometry.

of NS-2T. The PLQE value is more accurate and smaller than that reported in ref 12. We observe that the PLQE and τ_{PL} decrease in BC-2T with respect to NS-2T is mainly due to a strong reduction of the nonradiative decay time (τ_{nr}). The PLQE of BI-2T is very low and probably affected by different nonradiative channels.

IV. Discussion

Theoretical calculations show that the NS-2T has a complex electronic structure. The HF orbitals can be divided into orbitals localized on the bithiophene, orbitals localized on the succinimidyl group, and orbitals delocalized on the whole molecule. Also some low-lying Rydberg orbitals (e.g., the LUMO, not reported in Figure 2) can be recognized, due to the diffuse basis set employed. The excited states, both singlets and triplets, are highly correlated and are often characterized by at least two single-particle transitions.

For all the excited states one of the single-particle transitions is from an orbital localized on the bithiophene (succinimidyl) to an orbital localized on the succinimidyl (bithiophene). This feature might suggest that the excitations of NS-2T are of a charge-transfer character, but a more detailed analysis shows that this is not the case. In Figure 8 we report the plot of the difference between the S_2 (optically active) excited-state density and the ground-state density of NS-2T as computed at the CC2 level.

The differential density is completely localized on the bithiophene and on the C−O group, while no density appears on the succinimidyl ring. So there is no net charge separation. The charge transfer induced by the HOMO → LUMO + 1 transition is canceled by the HOMO → LUMO + 3 transition, so that the final result is a transition localized on the bithiophene.

This fact is also demonstrated by the invariance of the geometry of the succinimidyl group upon excitation. The same considerations also hold for S_1, which, despite the HOMO − 6 → LUMO + 1 transition, is described by a transition density localized on the succinimidyl group with no charge-transfer signature.

Even if there is no net charge separation in NS-2T, experimental results show a non-negligible (100 meV) shift of the PL main peak with the solvent polarity. In Table 6 the computed dipole moments of NS-2T are reported in the ground and excited states.

Most of the magnitude of the dipole is due to the component along the molecular axis, and only a little contribution is due to the perpendicular component. The origin of a large dipole in NS-2T can be traced back to the C−O group effect and to the acceptor nature of the oxygen atom. However, the effect of the nitrogen atom seems to compensate for that of the oxygen atom so that the O−N group plays a more minor role than the C−O group. Both CC2 and TD-DFT predict a much larger dipole in the excited state. As shown in Table 8 the emission energy decreases as the dielectric constant of the solvent increases. This effect is correctly related to the increased dipole moment in the excited state with respect to the ground state.[69]

In TD-DFT calculations (see right column of Table 1) we observe that S_1 is a pure charge-transfer state characterized almost completely as a HOMO → LUMO transition. For this state we can expect, except for a small contribution of the HF exchange in the hybrid kernel, the matrix elements of the TD-DFT kernel to vanish; thus the S_1 excitation energy is largely underestimated, and it almost coincides with the Kohn−Sham single-particle gap.[33] This observation is confirmed by calculations made using a Becke−Perdew[49,50] XC functional where half a dozen ghost states (Figure 9) appear below the true states due to the neglect of any nonlocal exchange in the Becke−Perdew kernel. Figure 9 also reports the results obtained with the LHFX approach, i.e., a TD-DFT calculation with the Becke exchange kernel using self-interaction-free Kohn−Sham orbitals and eigenvalues, obtained with the localized Hartree−Fock (LHF) approach.[52,53] The LHF Kohn−Sham potential is not only asymptotically correct, but it is self-interaction-free.[52] Thus the LHFX method can correctly treat Rydberg excitations but, because of the semilocal TD-DFT kernel, cannot properly describe CT excitations. By comparing the Becke−Perdew (B−P) and the LHFX results in Figure 9, we can estimate the effects that a correct Kohn−Sham (KS) potential has on excitation energies without considering TD-DFT coupling contributions. The lowest CT state increases by less than 0.3 eV going from B−P to LHFX due to the increased KS gap. A much larger effect is instead present going from B−P to B3LYP; in this case the lowest CT state is increased by about 1 eV, whereas transition localized on the bitiophene (indicated by "B" in Figure 9) increases only about 0.3 eV. These results show that by using a self-interaction-free/asymptotically correct KS potential the TD-DFT excitation energies are improved, but the effects of a nonlocal kernel are much larger. Similar conclusions were found in refs 33 and 70.

In Table 1, the S_1 state has no equivalent in the CC2 results. Thus we can consider S_1 as a ghost state, due to the XC kernel approximation. The presence of such a ghost state does not affect optical properties such as absorption spectra. In fact its oscillator strength is vanishingly small, and thus it does not contribute to the absorption spectra. However, ghost states completely modify the photophysical description, e.g., a optically forbidden lowest singlet state would mean quenching of the PL. Moreover, ghost states are present in the triplet spectrum, which then can be strongly corrupted and cannot be used for the description of photophysical properties (section IV.C).

A. Binding to Biomolecules. Theoretical calculations show that the BC-2T has an electronic structure that closely resembles that of isolated bithiophene. The occupied orbitals (Figure 2) do not change much after binding, and it is still possible to identify, among the orbitals appearing in the main single-particle transitions characterizing the excited states, orbitals localized on the bithiophene (HOMO) and orbitals localized on the substituent group (HOMO − 6 in NS-2T and HOMO − 5 in BC-2T). On the contrary the binding to a biomolecule has a strong effect on virtual orbitals. We can compare the LUMO + 1 and LUMO + 3 of NS-2T with the LUMO + 3 and LUMO + 6 of BC-2T to see that in BC-2T the orbital density is more localized on the bithiophene.

The excited states of BC-2T are characterized by many single-particle transitions, and it is difficult to identify the character of the excited state. Nevertheless, by inspection of the single-particle transitions, we can relate the first singlet state of BC-2T with the second singlet state of NS-2T and the second singlet

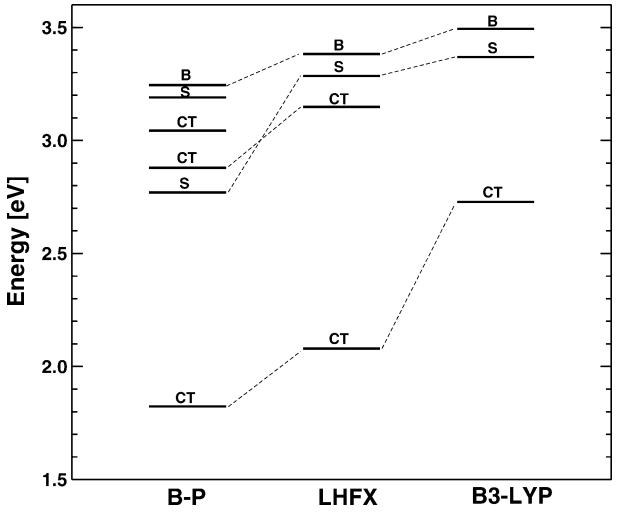

Figure 9. TD-DFT singlet excitation energy levels of NS-2T, up to the optically active one (B), computed using the Becke−Perdew (B−P) and the B3LYP XC functional and the LHFX approach (see text for details). For each level the character of the excitation is reported: S for excitation localized on the succinimidyl group, B for excitation localized on the bithiophene group, CT for a charge-transfer excitation.

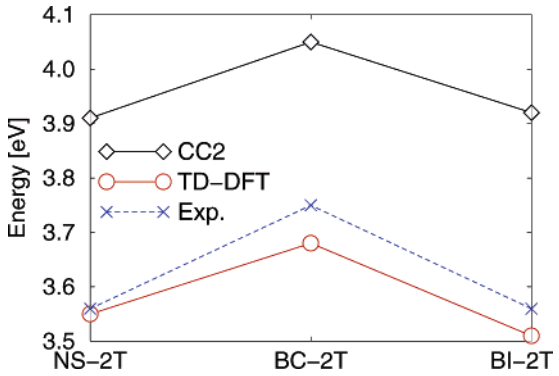

Figure 10. Comparison between CC2, TD-DFT, and the experimental absorption peak in dichloromethane solution.

state of BC-2T with the first singlet state of NS-2T. The reason that in BC-2T the excited states have a higher energy and appear in reverse order with respect to the excitations of NS-2T may be traced back to the greater weight in BC-2T excited states of transitions to higher orbitals and to the greater localization of virtual orbitals of BC-2T on bithiophene.

The origin of the localization of virtual orbitals deserves some more consideration. While the occupied orbitals show a common behavior in all three molecules, the virtual orbitals are more dependent on the presence of different functional groups. A major role is played by the oxygen atoms, which are well-known to attract charge in the virtual orbitals. In NS-2T the presence of three oxygen atoms in the C(O)−NH−succinimidyl group causes the electronic density to be strongly attracted by this group. As a consequence, the LUMO + 1 is spread over the entire molecule, and the LUMO + 3 is mostly localized on the succinimidyl group. In BI-2T, only one oxygen atom is present, and the effect is less strong. The LUMO + 2 is mainly localized on the bithiophene, but the LUMO + 6 is still mostly localized on the C−O group. In BC-2T again we have one oxygen atom, but its effect seems to be compensated for by the presence of the nitrogen atom. The virtual molecular orbitals thus are more localized on the bithiophene segment of the molecule.

B. Comparison with Experiments. In Figure 10 we compare the experimental absorption peak and the theoretical excitation for the optically active states for the three systems. We note that *trends* between different systems are very well predicted by both CC2 and TD-DFT. The excitation energy of BC-2T is predicted to be about 0.2 eV higher than that of NS-2T. This is due to the presence of oxygen atoms in the latter. In BC-2T the presence of the N−H group cancels the effect of the acceptor group of C−O. This is indeed confirmed by calculations on BI-2T (in which no N−H group is present), which has an excitation energy close to that of NS-2T. The blue shift in absorption energies going from NS-2T to BC-2T can be traced back to orbital energies, and it is easier to consider TD-DFT results as they are more easily described in terms of single-particle transitions. In NS-2T the optically active state is characterized by HOMO → LUMO + 1 while in B2-2T the transition is HOMO → LUMO. From from NS-2T to BC-2T, the HOMO energy increases by 0.309 eV, but the energy of the corresponding unoccupied orbital increases more (0.465 eV), meaning that the KS gap and thus the excitation energy are increasing.

However, when comparing *absolute values*, we note that the CC2 results are blue-shifted with respect TD-DFT by about 0.3 eV. This difference is related to the different approximations in the two methods, and similar differences were also found in oligothiophenes.[28] When comparing theoretical absolute values and experimental results, we must point out that (1) calculations are performed in empty space (i.e., the gas phase) while experimental measurements are performed in solution, and the latter are usually red-shifted (by about 0.1 eV) with respect to the gas-phase, and (2) we compute electronic vertical excitation energies while experimental measurements are related to the band maximum in solution where no vibronical replicas are visible, so that the band maximum can easily underestimate the vertical excitation energy (by about 0.1 eV). Thus we can conclude that *both* TD-DFT and CC2 are in very good agreement (by about 0.1−0.2 eV) with measurements within the experimental accuracy.

While absorption energies show significant difference among the systems, the *same emission energies* for all the three systems are predicted by both CC2 and TD-DFT, about 3.4 and 3.1 eV for CC2 and TD-DFT, respectively. This is in good agreement with the experimental measurements, where all the emission peaks are at about 3.0 eV. (Deviations less that 60 meV are present.) The equivalence of emission energies can be explained as follows.

In the excited-state geometry, all the optically active transitions are HOMO → LUMO. As it can be seen in Figure 4, the HOMO does not change its shape among the three systems; the same is true for the LUMO. Both orbitals are completely localized on the bithiophene segment, and they are very close to the isolated bithiophene, as previously observed, with the exception of the contribution on the C−O, which is almost equivalent in all the systems. While wave functions do not change among the systems, the orbitals energies are instead affected by the potentials of the substituent atoms, in particular oxygen and nitrogen. In fact the HOMO energy increases going from NS-2T to BC-2T and decreases going from BC-2T and NS-2T. The key point is that also the LUMO energies are modified *in the same way* as for the HOMO, meaning that the single-particle gap and thus excitation energies remain almost unchanged among the systems.

C. Photophysical Considerations. The main nonradiative decay path in unsubstituted oligothiophenes is known to be intersystem crossing (ISC).[28,71−73] A quantitative analysis of ISC requires the calculation of the singlet/triplet potential surfaces and the spin−orbit coupling from S_1 to the triplet manifold.[74−76]

We here describe qualitatively the ISC rate as a function of the S_1-T_n energy separation,[42,71,72,77−79] T_n being the triplet state closer in energy to S_1. This approximation is valid because the ISC rate decreases exponentially as the singlet−triplet gap increases.[74] It is important that the energy levels are computed at the correct geometry, i.e., the first singlet excited-state minimum.[42,72] The analysis of the triplet manifold reported in Tables 4 and 5 allows us to make some considerations of the PLQE.

Concerning NS-2T, T_1 has very low energy and thus does not contribute to the intersystem crossing process. The second triplet state is the closest to S_1, and the energy difference between T_2 and S_1 is −0.28 eV (Table 4). This value is higher than that computed at the same level of theory for other oligothiophenes,[28] so that we can expect that the ISC rate to be of minor importance, explaining the quite high PLQE. We note that the experimental PLQE of bithiophene is as low as 1%,[80] due to the very high ISC rate.[72] After binding to biomolecules (i.e., in the BC-2T system), the experimental PLQE and PL decay times strongly decrease. This can be explained in the same way by considering the decrease of the S_1-T_2 energy gap (−0.20 eV). However, the computed singlet−triplet splitting is probably not sufficient for a complete justification of PLQE differences. For BC-T2 other nonradiative decay channels might be important, such as the internal conversion due to the presence of the flexible carbonyl chains. However, these degrees of freedom of the flexible chains will be not present in a real biological system, where thus we can expect larger PLQE. Indeed preliminary PL measurements[12] show quite high PL for the TSE class in real operative biological conditions.

The photophysics of BI-2T is quite different. Theoretical results predict the second triplet below the first singlet, which means a very high ISC rate, supporting the extremely low PLQE. Moreover, the experimental time-resolved PL signal is not exponential, meaning that various decay channels are present.

V. Conclusions

In this work, we have analyzed the electronic and optical properties 5-*N*-succinimidyl-2,2′-bithiophene, a representative system for the oligothiophene *N*-succinimidyl esters class of biomarkers. We have performed CC2 and TD-DFT theoretical calculations in the ground and excited states and compared the results to optical measurements. We found that TD-DFT can be used to describe these systems, but validation using a correlated approach has been necessary due the presence of charge-transfer transitions. TD-DFT and CC2 predict absorption and emission energies very close to those of the experimental results. CC2 overestimates TD-DFT results by about 0.3 eV.

When covalently bound to a biomolecule, the succinimidyl group is replaced by a C(O)−NH group. We found experimentally and theoretically that such a replacement causes a *blue shift in the absorption spectrum* of about 0.2 eV, but no shifts are found in the photoluminescence spectra. In addition the binding to a biomolecule causes a decrease of the PLQE, in qualitative agreement with the decreased S_1-T_2 energy splitting.

The results presented in this work can be used to analyze how chemical binding to biomolecules might change the optical and photophysical properties of biomarkers. Of course, an accurate analysis in the biological environment (i.e., in water) and with real biosystems is required for a more complete understanding of the properties of biomarkers.

Acknowledgment. We thank R. Ahlrichs for providing the TURBOMOLE program package and G. Aloisio for his support. Calculations were performed at the CACT-ISUFI (Lecce).

References and Notes

(1) Bruchez, M., Jr.; Moronne, M.; Gin, P.; Weiss, S.; Alivisatos, P. *Science* **1998**, *281*, 2013.
(2) Oldham, P. B.; McCarrol, M. E.; McGown, L. B.; Warner, I. M. *Anal. Chem.* **2000**, *72*, 197R.
(3) Barbarella, G.; Zambianchi, M.; Pudova, O.; Palladini, V.; Ventola, A.; Cipriani, F.; Gigli, G.; Cingolani, R.; Citro, G. *J. Am. Chem. Soc.* **2001**, *123*, 11600.
(4) Barbarella, G. *Chem.—Eur. J.* **2002**, *8*, 5072.
(5) Sotgiu, G.; Zambianchi, M.; Barbarella, G.; Aruffo, F.; Cipriani, F.; Ventola, A. *J. Org. Chem.* **2003**, *68*, 1512.
(6) Nilson, K. P. R.; Inganas, O. *Nat. Mater.* **2003**, *2*, 419.
(7) Wu, X.; Liu, H.; Haley, K. N.; Treadway, J. A.; Larson, J. P.; Ge, N.; Peale, F.; Bruchez, M. P. *Nat. Biotechnol.* **2003**, *21*, 41.
(8) Jaiswal, J. K.; Mattoussi, H.; Mauro, J. M.; Simon, S. M. *Nat. Biotechnol.* **2003**, *21*, 47.
(9) Dorè, K.; Dubus, S.; Ho, H. A.; Lèvesque, I.; Brunette, M.; Corbeil, G.; Boivin, M.; Bergron, M. G.; Boudreau, D.; Leclerc, M. *J. Am. Chem. Soc.* **2004**, *126*, 4240.
(10) Cao, X.; Cui, Y.; Levenson, R. M.; Chung, L. W. K.; Nie, S. *Nat. Biotechnol.* **2004**, *22*, 969.
(11) Derfus, A. M.; Chan, W. C.; Bathia, S. N. *Nano Lett.* **2004**, *4*, 11.
(12) G. Barbarella, G.; M. Zambianchi, M.; A. Ventola, A.; E. Fabiano, E.; F. Della Sala, F.; G. Gigli, G.; M. Anni, M.; A. Bolognesi, A.; L. Polito, L.; M. Naldi, M.; M. Capobianco, M. *Bioconjugate Chem.* **2006**, *17*, 58.
(13) Fichou, D. *Hanbook of Oligo and Polythiophenes*; Wiley-VCH: New York, 1999.
(14) Horowitz, G.; Delannoy, P.; Bouchriha, H.; Deloffre, F.; Fave, J. L.; Garnier, F.; Hajlaoui, R.; Heyman, M.; Kouki, F.; Valat, P.; Wintgens, V.; Yassar, A. *Adv. Mater.* **1994**, *6*, 752.
(15) Gigli, G.; Barbarella, G.; Favaretto, L.; Cacialli, F.; Cingolani, R. *Appl. Phys. Lett.* **1999**, *75*, 439.
(16) Shirota, Y.; Kinoshita, M.; Noda, T.; Okumoto, K.; Ohara, T. *J. Am. Chem. Soc.* **2000**, *122*, 11021.
(17) Mazzeo, M.; Vitale, V.; Della Sala, F.; Anni, M.; Barbarella, G.; Favaretto, L.; Sotgiu, G.; Cingolani, R.; Gigli, G. *Adv. Mater.* **2005**, *17*, 34.
(18) Zavelani-Rossi, M.; Lanzani, G.; De Silvestri, S.; Anni, M.; Gigli, G.; Cingolani, R.; Barbarella, G.; Favaretto, L. *Appl. Phys. Lett* **2001**, *79*, 4082.
(19) Garnier, F.; Horowitz, G.; Fichou, D.; Peng, X. *Adv. Mater.* **1990**, *2*, 592.
(20) Dodabalapur, A.; Katz, H. E.; Torsi, L.; Haddon, R. C. *Science* **1995**, *269*, 1560.
(21) Dimitrakopoulos, C. D.; Malenfant, P. R. L *Adv. Mater.* **2002**, *14*, 99.
(22) Haugland, R. P. *Handbook of Fluorescent Probes and Research Products*; Molecular Probes: Eugene, OR, 2001.
(23) Banks, P. R.; Paquette, D. M.; *Bioconjugate Chem.* **1995**, *6*, 447.
(24) Helgaket, T.; Jørgensen, P.; Olsen. J. *Molecular Electronic-Structure Theory*; John Wiley & Sons: Chichester, U. K., 2000.
(25) Christiansen, O.; Koch, H.; Jørgensen, P. *Chem. Phys. Lett.* **1995**, *243*, 409.
(26) Hättig, C.; Weigend, F. *J. Chem. Phys.* **2002**, *113*, 5154.
(27) Fabiano, E.; Della Sala, F.; Cingolani, R. *Phys. Status Solidi C* **2004**, *1*, 539.
(28) Fabiano, E.; Della Sala, F.; Cingolani, R.; Weimer, M.; Görling, A. *J. Phys. Chem. A* **2005**, *109*, 3078.
(29) Hättig, C. *J. Chem. Phys.* **2003**, *118*, 7751.
(30) Kohn, A.; Hättig, C. *J. Chem. Phys.* **2003**, *119*, 5021.
(31) Casida, M. E.; Gutierrez, F.; Guan, J.; Gadea, F.-X.; Salahub, D.; Daudey, J.-P. *J. Chem. Phys.* **2000**, *113*, 7062.
(32) Jamorski, C.; Foresman, J. B.; Thilgen, C.; Lüthi, H.-P. *J. Chem. Phys.* **2002**, *116*, 8761.
(33) Dreuw, A.; Weisman, J. L.; Head-Gordon, M. *J. Chem. Phys.* **2003**, *119*, 2943.
(34) Tozer, D. J. *J. Chem. Phys.* **2003**, *119*, 12697.
(35) Dreuw, A.; Head-Gordon, M. *J. Am. Chem. Soc.* **2004**, *126*, 4007.
(36) Gritsenko, O.; Baerends, E. J. *J. Chem. Phys.* **2004**, *121*, 655.
(37) Tawada, Y.; Tsuneda, T.; Yanagisawa, S.; Yanai, T.; Hirao, K. *J. Chem. Phys.* **2004**, *120*, 8425.
(38) Maitra, N. T. *J. Chem. Phys.* **2005**, *122*, 234104.
(39) Becke, A. D. *J. Chem. Phys.* **1993**, *98*, 5648.
(40) Vitale, V.; Della Sala, F.; Cingolani, R. *Phys. Status Solidi C* **2004** *1*, 555.
(41) Furche, F.; Ahlrichs, R. *J. Chem. Phys.* **2002**, *117*, 7433.
(42) Raganato, M. F.; Vitale, V.; Della Sala, F.; Anni, M.; Cingolani, R.; Gigli, G.; Favaretto, L.; Barbarella, G.; Weimer, M.; Görling, A. *J. Chem. Phys.* **2004**, *121*, 3784.
(43) Hättig, C.; Weigend, F. *J. Chem. Phys.* **2000**, *113*, 5154.
(44) Weigend, F.; Häser, M.; Patzelt, H.; Ahlrichs, R. *Chem. Phys. Lett*, **1998**, *294*, 143.

(45) Schäfer, A.; Hüber, C.; Ahlrichs, R. *J. Chem. Phys.* **1994**, *100*, 5829.
(46) Dunning, T. H., Jr. *J. Chem. Phys.* **1989**, *90*, 1007.
(47) Weigend, F.; Köhn, A.; Hättig, C. *J. Chem. Phys.* **2002**, *116*, 3175.
(48) Jansen, C. L.; Nielsen, I. M. B. *Chem. Phys. Lett.* **1998**, *290*, 423.
(49) Becke, A. D. *Phys. Rev. A* **1988**, *38*, 3098.
(50) Perdew, J. P. *Phys. Rev. B* **1986**, *33*, 8822.
(51) Della Sala, F.; Görling, A. *J. Chem. Phys.* **2003**, *118*, 10439.
(52) Della Sala, F.; Görling, A. *J. Chem. Phys.* **2001**, *115*, 5718.
(53) Della Sala, F.; Görling, A. *J. Chem. Phys.* **2002**, *116*, 5374.
(54) Della Sala, F.; Görling, A. *Int. J. Quantum Chem.* **2003**, *91*, 131.
(55) Ahlrichs, R.; Bär, M.; Häser, M.; Horn, H.; Kölmel, C. *Chem. Phys. Lett.* **1999**, *162*, 165.
(56) Häser, M.; Ahlrichs, R. *J. Comput. Chem.* **1989**, *10*, 104.
(57) Horn, H.; Weiass, H.; Häser, M.; Ehrig, M.; Ahlrichs, R. *J. Comput. Chem.* **1991**, *12*, 1058.
(58) Treutler, O.; Ahlrichs, R. *J. Chem. Phys.* **1995**, *102*, 346.
(59) Arnim, M. V.; Ahlrichs, R. *J. Chem. Phys.* **1999**, *111*, 9183.
(60) Weiss, H.; Ahlrichs, R.; Häser, M. *J. Chem. Phys.* **1993**, *99*, 1262.
(61) Bauernschmitt, R.; Ahlrichs, R. *J. Chem. Phys.* **1996**, *104*, 9047.
(62) Treutler, O.; Ahlrichs, R. *Chem. Phys. Lett.* **1997**, *264*, 573.
(63) Grimme, S.; Furche, F.; Ahlrichs, R. *Chem. Phys. Lett.* **2002**, *361*, 321.
(64) Furche, F.; Ahlrichs, R. *J. Chem. Phys.* **2002**, *117*, 7433.
(65) Hättig, C.; Hald, K. *Phys. Chem. Chem. Phys.* **2002**, *4*, 2111.
(66) Hättig, C.; Köhn, A. *J. Chem. Phys.* **2002**, *117*, 6939.
(67) Köhn, A.; Hättig, C. *J. Chem. Phys.* **2003**, *118*, 7751.
(68) Anni, M.; Della Sala, F.; Raganato, M. F.; Fabiano, E.; Cingolani, R.; Gigli, G.; Görling, A. *J. Phys. Chem. B* **2005**, *109*, 6004.
(69) Lami, H.; Glasser, N. *J. Chem. Phys.* **1986**, *84*, 597.
(70) Weimer, M.; Hieringer, W.; Della Sala, F.; Görling, A. *Chem. Phys.* **2005**, *209*, 309.
(71) Belijonne, D.; Cornil, J.; Friend, R. H.; Janssen, R. A. J.; Brédas, J. L. *J. Am. Chem. Soc.* **1996**, *118*, 6453.
(72) Rubio, M.; Merchan, M.; Pou-Amerigo, R.; Orti, E. *ChemPhysChem* **2004**, *4*, 1308.
(73) Yang, J. P.; Paa, W.; Rentsch, S. *Chem. Phys. Lett.* **2000**, *320* 665.
(74) Englman, R.; Jortner, J. *Mol. Phys.* **1970**, *18*, 145.
(75) Kleinschmidt, M.; Tatchen, J.; Marian, C. M. *J. Comput. Chem.* **2002**, *23*, 824.
(76) Tunell, I.; Rinkevicius, Z.; Vahtras, O.; Saek, P.; Helgaker, T.; Ågren, H. *J. Chem. Phys.* **2003**, *119*, 11024.
(77) Burin, A. L.; Ratner, M. A. *J. Chem. Phys.* **1998**, *109*, 6092.
(78) Gigli, G.; Della Sala, F.; Lomascolo, M.; Anni, M.; Barbarella, G.; Di Carlo, A.; Lugli, P.; Cingolani, R. *Phys. Rev. Lett.* **2001**, *86*, 167.
(79) Della Sala, F. Heinze, H. H. Görling, A. *Chem. Phys. Lett.* **2001**, *339*, 343.
(80) Becker, R. S.; de Melo, J. S.; Macanita, A. L.; Elisei, F. *J. Phys. Chem.* **1996**, *100*, 18683.